The cubic to rhombohedral phase transition of

Pb(Zn$_{1/3}$Nb$_{2/3}$)O$_3$: a high-resolution X-ray diffraction study

on single crystals.

A. Lebon[*], H. Dammak, G. Calvarin, I. Ould Ahmedou

Structures, Propriétés et Modélisation des Solides, UMR 8580, CNRS - Ecole Centrale

Paris, Grande Voie des Vignes, 92295 Châtenay-Malabry Cedex, France.

Short title: Study of the phase transition in the relaxor ferroelectric PZN by x-ray
diffraction.

---

[*] Correspondences should be sent to A. Lebon, current address: Festkörperforshung, Max Planck Institut, 1,

Heisenbergstrasse, 70569 Stuttgart.

e-mail: a.lebon@fkf.mpg.de

ABSTRACT

The cubic to rhombohedral (C-R) phase transition of the ferroelectric-relaxor $Pb(Zn_{1/3}Nb_{2/3}O_3)$ (PZN) is investigated using high-resolution X-ray diffraction on single crystals. The phase transition is diffuse and spreads over the temperature range $T_{CR} = 385 \pm 5$ K $- T_R = 325 \pm 5$ K. Below T_{CR}, the cubic phase transforms progressively into rhombohedral domains the average size of which, about 60-70 nm in the [111] direction, remains unchanged as temperature is lowered, so no growth of the R-phase is observed. At T_R, the nanometric R-domains fully pave the crystal but structural mismatches between adjacent domains generate stresses, which increase as temperature is lowered. The anomalous broadening of diffraction peaks of the R-phase, which originates from size and strain effects, can be suppressed by applying a dc-electric field, along the [111] direction, which transforms the polydomain state into a rhombohedral quasi-monodomain state.

1. INTRODUCTION

Relaxor ferroelectrics were first synthesized in the late fifties and since that time they attracted lots of attention because of the unusual behaviour of their dielectric permittivity [1]. In fact, they display a significant dielectric anomaly characterized by strong frequency dispersion and no macroscopic spontaneous polarization. Many of these materials are lead based perovskite with general formula PbBB'O_3 (B = Mg^{2+}, Zn^{2+}, Ni^{2+}, Sc^{3+}... ; B' = Nb^{5+}, Ta^{5+}, W^{6+}...). The most documented relaxor Pb($Mg_{1/3}Nb_{2/3}$)O_3 (PMN) retains a cubic structure on average down to 5 K [2]. Pb($Zn_{1/3}Nb_{2/3}$)O_3 (PZN), which is isomorphous to PMN, exhibits as well the dielectric behavior of a relaxor ferroelectric, but it is characterized by a symmetry lowering towards a rhombohedral ferroelectric phase as shown in the early study of Yokomizo et al [3]. The cubic to rhombohedral (C-R) phase transition which occurs around T = 390 K does not coincide with the maximum of the dielectric permittivity (T_{max} = 405 K, f = 1 kHz) [4]. From optical observations carried out on single crystals Mulvihill et al [5] showed that the ferroelectric phase of PZN appears in a so-called microdomain state (<100 nm), which transforms into a macrodomain state under a dc electric field parallel to [111]. Moreover, from structural refinements of powder neutron diffraction patterns, Iwase et al [6] showed that the best results were obtained by assuming the coexistence of both cubic and rhombohedral phases below 550 K. The rhombohedral phase ratio reaches 40 % at room temperature. On the other hand, Raman scattering experiments carried out on PZN single crystal by Lebon et al [7] did not give evidence of phase coexistence above 390 K; in return, below this temperature a drastic increase of the intensity ratio $I_\perp/I_{//}$ of the Raman bands was observed and associated to the onset of a rhombohedral microdomain state.

In order to get a better characterization of the C-R phase transition of PZN an X-ray diffraction study was carried out on single crystals by means of a high-resolution diffractometer.

2. EXPERIMENTAL CONDITIONS

PZN single crystals were grown using a flux method with excess lead oxide. They were extracted from the flux with the aid of a warm 25% vol nitric acid solution [4,8]. Three yellow transparent crystals were oriented and cut according to the crystallographic planes (100), (110) and (111) using the Laue technique. The crystals, accordingly $3\times2\times0.5$ mm^3 platelets were polished on both surfaces, then annealed at 450° C in order to remove residual stresses.

The x-ray diffraction diagrams were recorded with a high accuracy 2-axes diffractometer in Bragg-Brentano geometry built up in the laboratory [9]. Diffraction angles were measured with a relative precision better than 0.002° (2Θ) owing to a photoelectric encoder connected to the rotation axis of the diffractometer. A graphite monochromator selected the Cu-K$_\beta$ wavelength ($\lambda = 0.139223$ nm) issued from an 18 kW rotating anode (Rigaku). Single crystals were fixed on a copper sample holder within a N$_2$ flow cryostat (230 - 470K) mounted upon a HUBER goniometric head.

3. RESULTS

Special care was taken to select Bragg reflections with high diffraction angles since they are more sensitive to any weak structural distortion. The (333), (330) and (005) reflections were selected and recorded from the three crystals respectively in the

temperature range 450-241 K. Figure 1 shows plots at T = 400 K and 300 K (RT). At RT, the peaks (333) and (330) are split while the peak (005) remains unique which is consistent with a rhombohedral symmetry as already reported in literature [3]. The anomalous broadening of peaks at RT, with respect to high temperature, will be discussed below. Figure 2 shows recordings of (333) peak at six selected temperatures. Down to 400 K, the single peak (figure 2a) corresponds to the cubic phase. At T = 370 K, an asymmetry is observed on the left side of the peak (figure 2a), asymmetry which turns into a shoulder at T = 351 K (figure 2b). At lower temperatures, two very distinct peaks, corresponding to the rhombohedral doublet $(333)_R$ and $(-333)_R$, are clearly evidenced. The progressive splitting of (333) indicates that the spontaneous C-R phase transition of PZN is diffuse in temperature. The temperature dependence of the full-width at quarter-maximum (FWQM) of (333) is shown in figure 3. FWQM slightly increases in the cubic phase then it abruptly jumps. The slope change takes place at 385 ± 5 K. A similar behaviour is also observed for the temperature dependence of the full-width at half-maximum (FWHM) of (005), (figure 3). So, T_{CR} = 385 ± 5K can be taken as the onset temperature of the C-R phase transition. In addition, a second slope change takes place at 325 ± 5 K, the significance of which will be discussed below.

In order to get further quantitative information about the structural features of the C-R phase transition, the (333) peak was fitted using pseudo-Voigt profile functions. Below T_{CR}, two components are fitted and the low angle component is assigned to the R-peak $(333)_R$. The temperature dependences of intensities and FWHM are shown in figures 4a and 4b respectively. The intensity of the R-component $(333)_R$ increases in the whole temperature range below T_{CR}, as the intensity of $(333)_C$ does in the C-phase (figure

4a). On the other hand, the intensity of the high angle component decreases from T_{CR} down to around 325K and further remains quasi constant. The FWHM of the R-component $(333)_R$ is quasi constant between T_{CR} and 325K but is much higher than the $(333)_C$ one, $0.30°$ against $0.17°$ (2Θ), (figure 4b). In return, in the temperature range T_{CR} - 325K, the FWHM of the high angle component increases from $0.17°$ to $0.30°$ (2Θ). Below 325K, the FWHM of both components are equal and increase in a similar way (figure 4b). These temperature dependences reveal a behaviour change, at $T_R = 325 \pm 5$ K, which can be related to the ending of the C-R phase transition. Thus, in the temperature range T_{CR}-T_R, the high angle component is the resultant of a summation of C-peak $(333)_C$ and of R-peak $(-333)_R$ which are closely superimposed. Just below T_{CR}, the contribution of the C-peak is predominant; in return, close above T_R and below this temperature the R-peak prevails.

The temperature dependence of the cell volume of PZN, derived from fits, is shown in figure 5. Again, a change of behaviour is observed in the temperature range T_{CR} - T_R. The volume of both C-phase (above T_{CR}) and R-phase (below T_R) decreases as temperature is lowered; however R-volume is higher, at T_{CR} $\Delta V/V = 0.06\%$ (figure 5). Thus, the C-R phase transition of PZN is weakly first order, which is consistent with the observed phase coexistence in the temperature range T_{CR} - T_R; in this range the cell volume dependence is meaningless (figure 5).

4. DISCUSSION

The temperature dependences of intensity (figure 4a) and FWHM (figure 4b) of the R-peak $(333)_R$, between T_{CR} and T_R, suggest that the C-phase transforms

progressively into nanometric R-domains quasi constant in size. The average size along the [111] direction could be calculated by means of the Scherrer formula [10], assuming that the instrumental width is equal to the $(333)_C$ FWHM in the C-phase. The estimated size of 60-70 nm for the R-domains is in qualitative agreement with the optical observations of Mulvihill et al [5] who evidenced ferroelectric domains of less than 100 nm in size. The onset of nanometric R-domains within the C-matrix has been also observed in PMN. However, for this latter, the transformation is not spontaneous, but time dependent when a dc electric field is applied along a [111] direction below a temperature $T_g = 230$ K: i.e. in the so-called glassy phase of PMN [11]. Moreover, as for PZN, nanometric R-domains nucleate within the C-phase with a constant average size of 70 nm in the [111] direction [12].[*]

At T_R the crystal is fully paved by nanometric R-domains, but stresses are generated inside the crystal because of structural mismatches between adjacent domains. Below T_R, structural mismatches increase correlatively to the rhombohedral distortion, as illustrated in figure 6 with the temperature dependence of rhombohedral angle alpha. Thus, below T_R a strain effect is superimposed to the size one which explains the increase of FWHM of both R-peaks $(333)_R$ and $(-333)_R$ The temperature dependence of (005) FWHM (figure 3) can also be explained by the contribution of both broadening effects. The broadening of R-phase peaks, generated by size and strain effects, can be suppressed by poling the crystal, under the condition that a sufficient electric field is applied along the direction of polarisation [111] [13]. This process transforms the nanometric polydomain state into a macroscopic quasi monodomain state as illustrated in figure 7 by

---

[*] The wrong value of R-domains size reported in reference [11] comes from a mistake in calculation [12].

the behaviour of the (333) Bragg reflection, where the R-peak $(333)_R$ is favoured by the dc electric field. This transformation of the domain state is accompanied by a decrease of both $(333)_R$ and (005) FWHM that recover their value of the C-phase (figure 1). These results confirm that the anomalous broadenings associated with the spontaneous C-R phase transition arise from the existence of a nanometric polydomain state.

The temperature dependence of the depolarisation ratio $I_\perp/I_{//}$ of the Raman spectra of PZN was measured with the same single crystal used for X-ray experiments [7]. This ratio was found to increase rapidly from T_{CR} to T_R, temperature where it approaches unity. This behaviour was assigned to a signature of the onset of ferroelectric microdomains.

5. CONCLUSION

In conclusion, our diffraction results reveal that the spontaneous C-R phase transition of PZN is first order and diffuse in temperature. The structural transformation takes place by a progressive nucleation of nanometric R-domains within the C-matrix, in the temperature range T_{CR}-T_R. The average size of R-domains remains unchanged in the whole temperature range investigated, so no growth of the R-phase is observed. The similar size lock-in observed in the first stage of the electric field induced C-R phase transition of PMN has very likely a common origin. In fact, a recent x-ray investigation of PMN and PZN using a synchrotron source showed that chemically ordered regions exist in both compounds [14]. These ordered regions are the sources of quenched random fields, which might explain why the R-domains cannot grow over a few tens of nanometers.

REFERENCES:

[1] G.A. Smolensky et al Sov. Phys. Solid. State **2**, 2584 (1961).

[2] P. Bonneau, P. Garnier, G. Calvarin, E. Husson, G.R Gavarri, A.W. Hewatt and A. Morell, J. Solid State Chem. **91**, 350 (1991).

[3] Y. Yokomizo, T. Takahashi, and S. Nomura, J. Phys. Soc. Jpn. **28**, 1278 (1970).

[4] I.A. Ould, PhD thesis, Ecole Centrale de Paris (1997).

[5] M.L. Mulvihill, L.E. Cross, W. Cao, K. Uchino, J. Am. Ceram. Soc. **80(6)**, 1462 (1997).

[6] T. Iwase, H. Tazawa, K. Fujishiro, Y. Uesu, Y. Yamada, Journal of Physics and Chemistry of Solids. **60**, 1419 (1999)

[7] A. Lebon, M. El Marssi, R. Farhi, H. Dammak, G. Calvarin. J. Appl. Phys. **89(7)**, 3947 (2001).

[8] M.L. Mulvihill, S.E. Park, G. Risch, Z. Li, K. Uchino, Jpn.J.Appl.Phys. **35**, 3984 (1996).

[9] J.F.Bérar, G.Calvarin, D.Weigel, J.Appl.Cryst.,**13**,201 (1980)

[10] A. Guinier, Théorie et technique de la radiocristallographie, p462 Dunod (1964).

[11] S. B. Vakhrushev, J.-M. Kiat and B. Dkhil, Solid. State. Com. **103**(8) p 477 (1997).

[12] B. Dkhil, PhD thesis Université Paris XI (1999).

[13] H. Dammak, A. Lebon, G. Calvarin, Ferroelectrics **235**, 151 (1999)

[14] Fanning. D.M, Robinson. I.K, Lu. X, Payne. D.A, Journal of Physics and Chemistry of Solids **61** p209(2000).

CAPTIONS:

Figure 1: Diffraction patterns at T = 400 K and **300 K** temperature of three Bragg reflections: a) (333), b) (330), and c) (005).

Figure 2: Temperature dependence of the diffraction peak (333) in the ranges: a) 450-370 K, b) 351-241 K.

Figure 3: Temperature dependences of (333) (FWQM) and (005) FWHM. Two slope changes are observed at $T_{CR} = 385 \pm 5$ K and $T_R = 325 \pm 5$ K.

Figure 4: Temperature dependence of intensities (4a) and (FWHM) (4b) of $(333)_C$, $(333)_R$ and $(-333)_R$ peaks. The indices C and R stand for the cubic and the rhombohedral phases.

Figure 5: Temperature dependence of the cell volume of PZN.

Figure 6: Rhombohedral distortion as a function of temperature below T_R.

Figure 7: Recordings from the same crystal of diffraction peaks (333) and (005) before (E = 0) and after poling, with an applied electric field along [111].
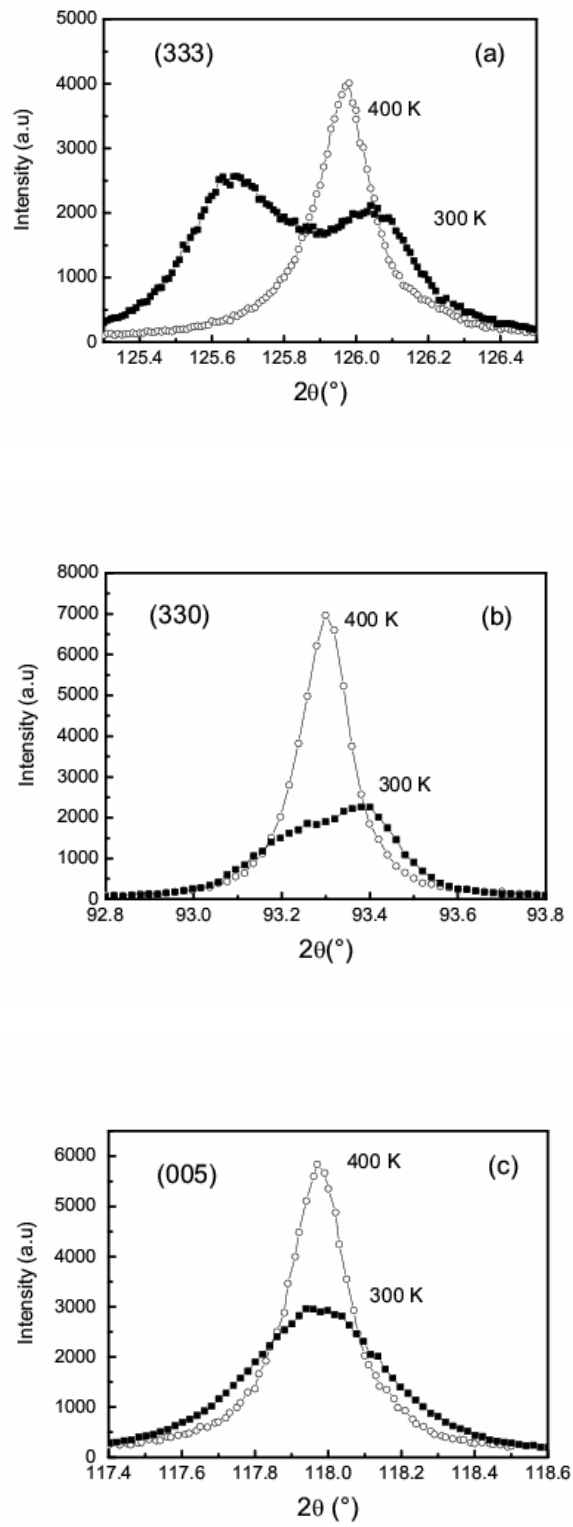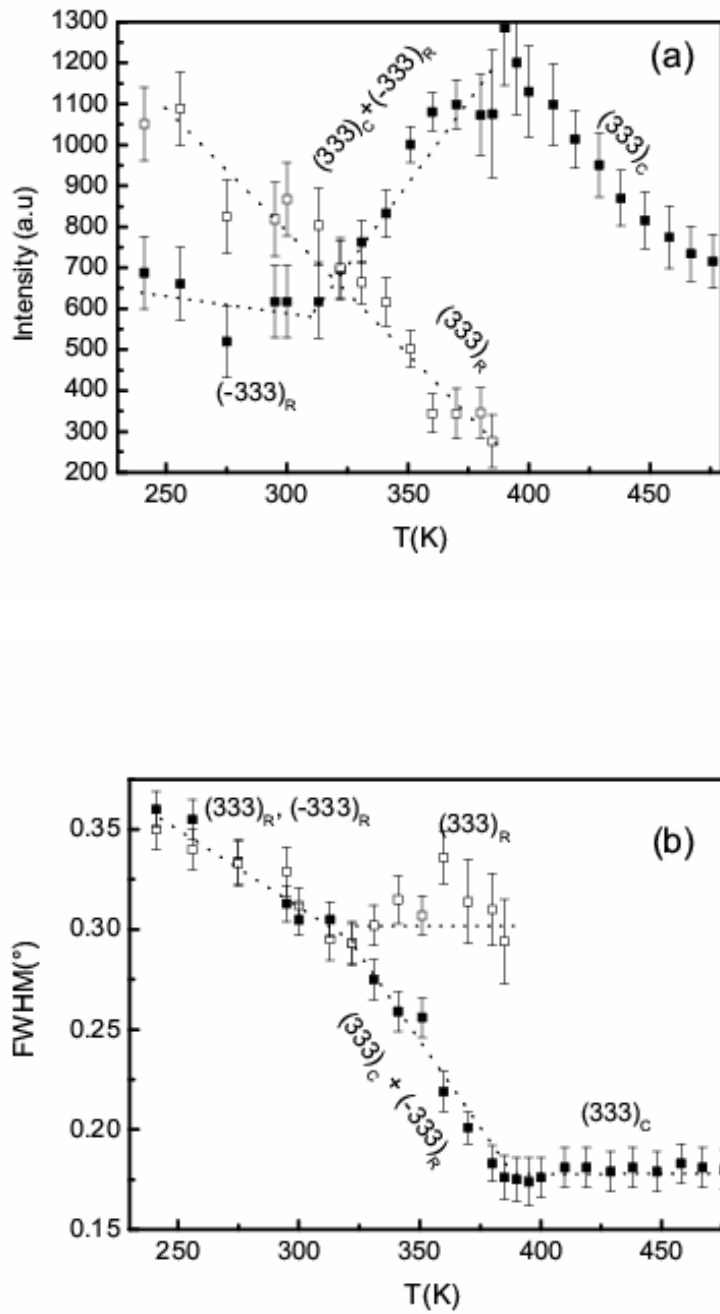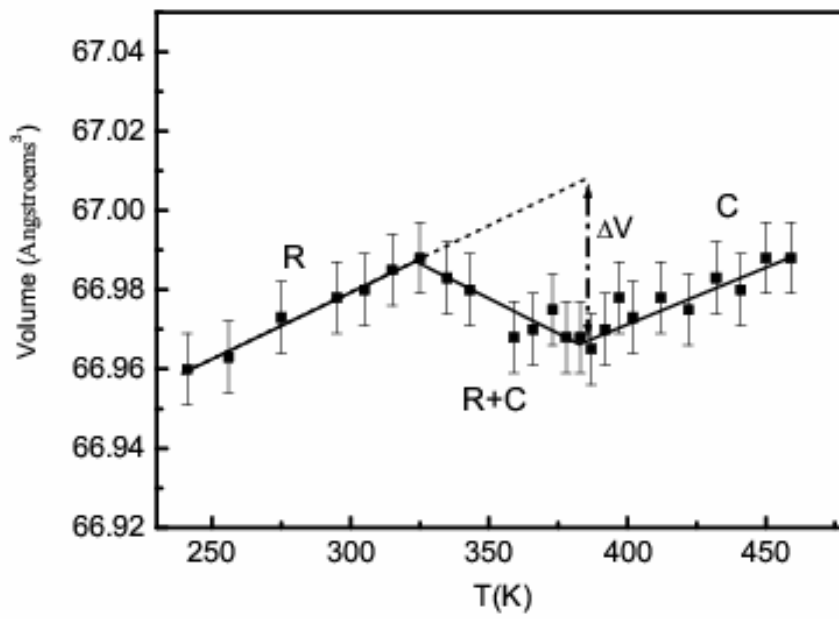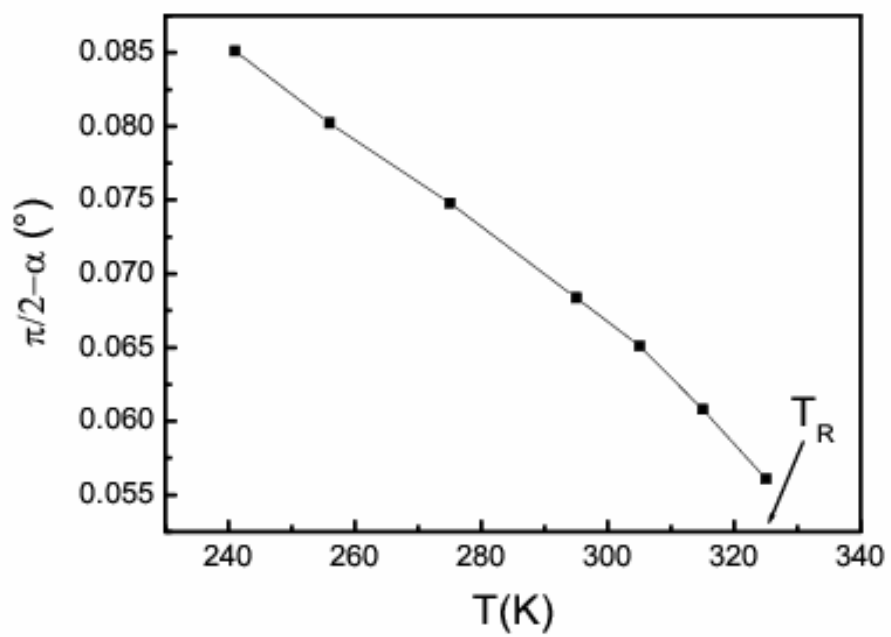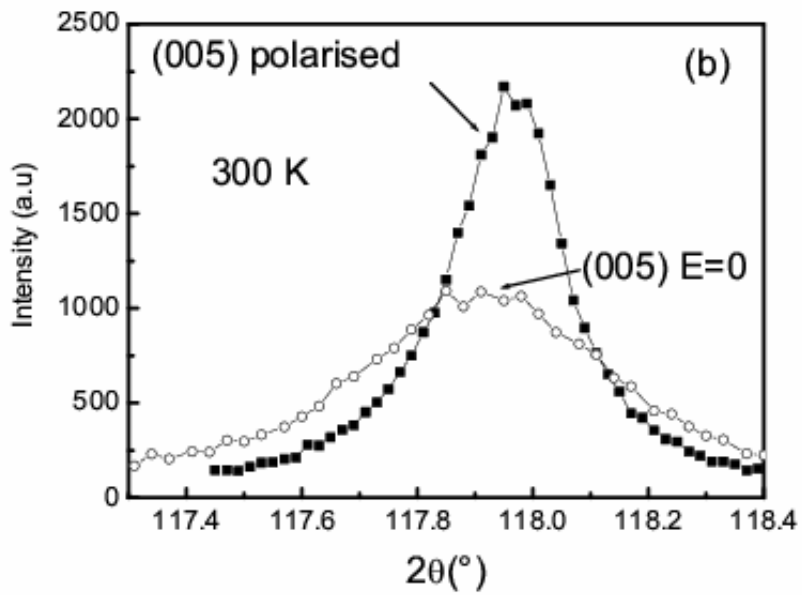
Figure 1
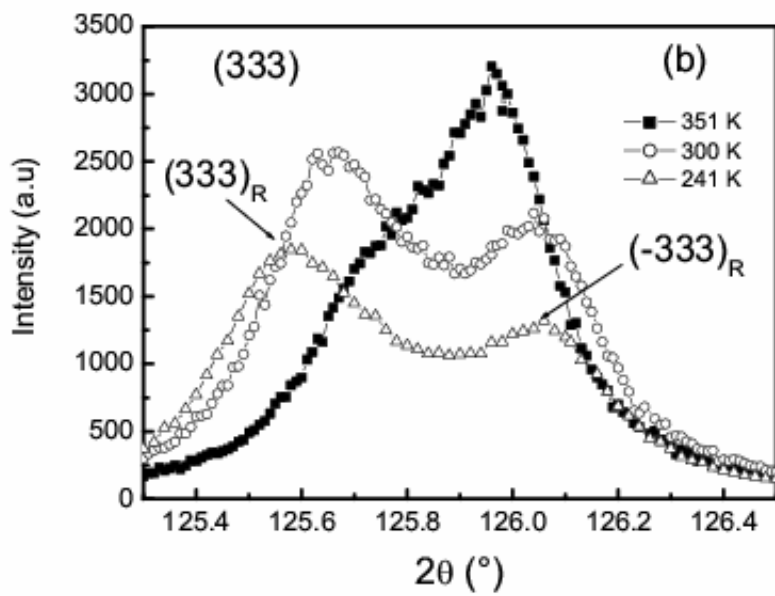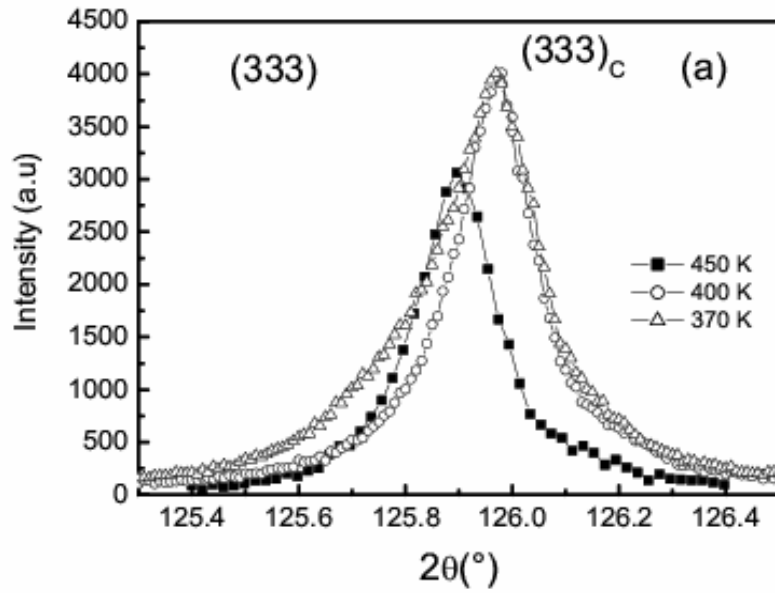
Figure 2
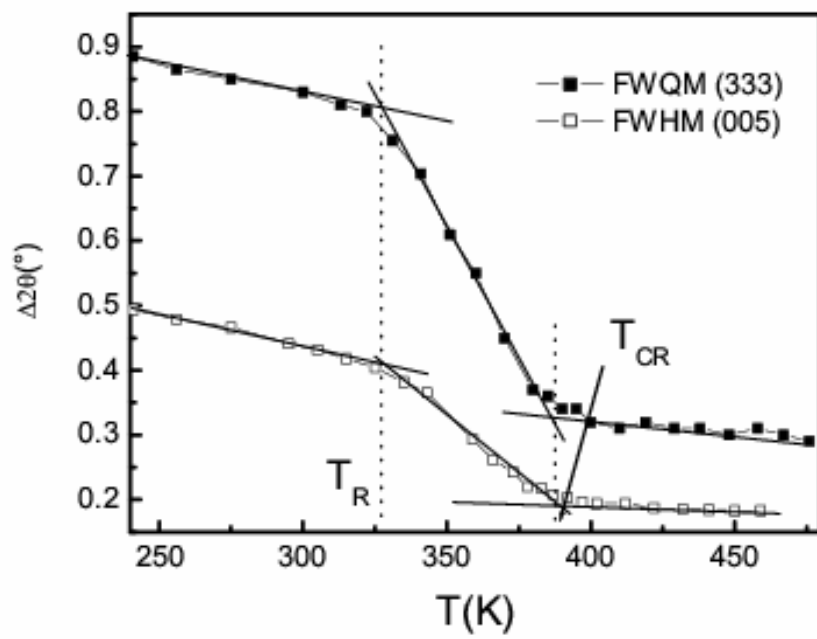
Figure 3

Figure 4

Figure 5

Figure 6

Figure 7